Electronic Supplementary Material (ESI) for Journal of Materials Chemistry C.


# Achieving ultrahigh dielectric breakdown strength in MgO-based ceramics by composite structure design

Chi Zhang, [ab] Ying Chen, *[ab] Mingxing Zhou, [ab] Xin Li, [a] Lei Wang, [ab] Liansheng Xia, [c] Yi Shen, [c] and Xianlin Dong, *[abd]

[a] *Key Laboratory of Inorganic Functional Materials and Devices, Shanghai Institute of Ceramics, Chinese Academy of Sciences, 588 Heshuo Road, Jiading District, Shanghai 201800, People's Republic of China*

[b] *Center of Materials Science and Optoelectronics Engineering, University of Chinese Academy of Sciences, 19 Yuquan Road, Shijinshan District, Beijing 100049, People's Republic of China*

[c] *Institute of Fluid Physics, China Academy of Engineering Physics, Mianyang 621900, People's Republic of China*

[d] *State Key Laboratory of High Performance Ceramics and Superfine Microstructure, Shanghai Institute of Ceramics, Chinese Academy of Sciences, 588 Heshuo Road, Jiading District, Shanghai 201800, People's Republic of China*

***Corresponding E-mail:*** chenying@mail.sic.ac.cn, xldong@mail.sic.ac.cn.

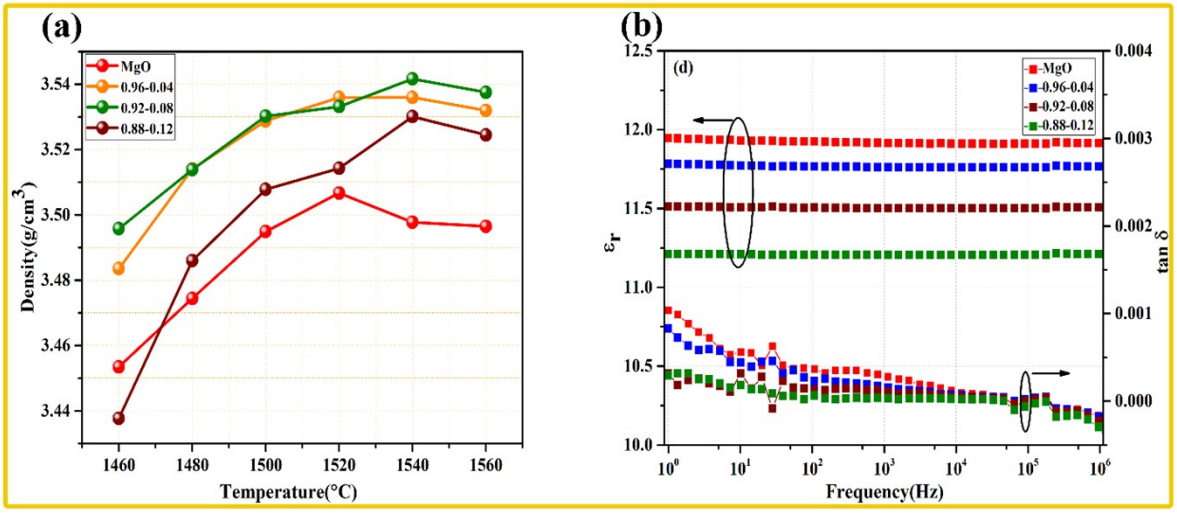


**Figure S1** (a) Density of (1-*x*)MgO-*x*$Al_2O_3$ ceramics sintered at different temperature measured by Archimedes method. (b) Dielectric frequency spectra of (1-*x*)MgO-*x*$Al_2O_3$ ceramics at room temperature.

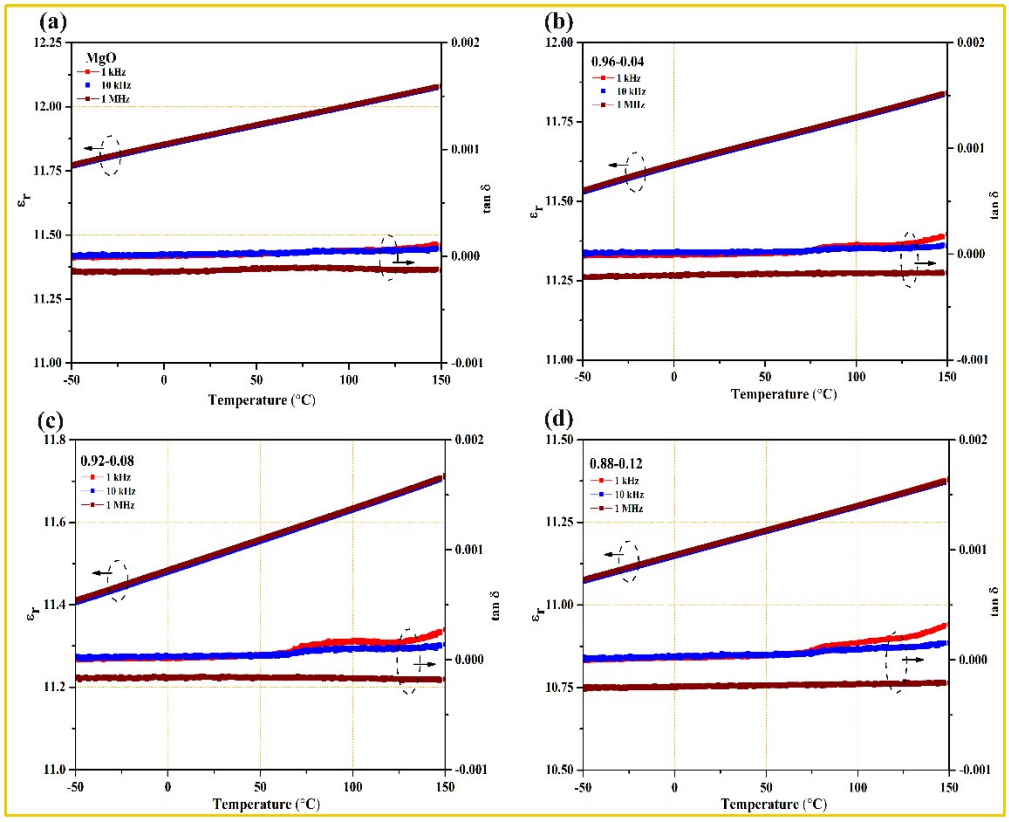


**Figure S2** Dielectric temperature spectra tested from -50 °C -150 °C at different frequencies of (a) MgO, (b) 0.96MgO-0.04$Al_2O_3$, (c) 0.92MgO-0.08$Al_2O_3$ and (d) 0.88MgO-0.12$Al_2O_3$.

As a kind of typical linear dielectric, all sintered samples show good frequency stability in Fig. S1b with tan δ < 0.001 from 1 Hz to 1 MHz. The addition of $Al_2O_3$ leads to the decrease in permittivity and dielectric loss while the latter is owing to space charge polarization relevant to their microstructure. Furthermore, good temperature stability are beneficial for practical application.

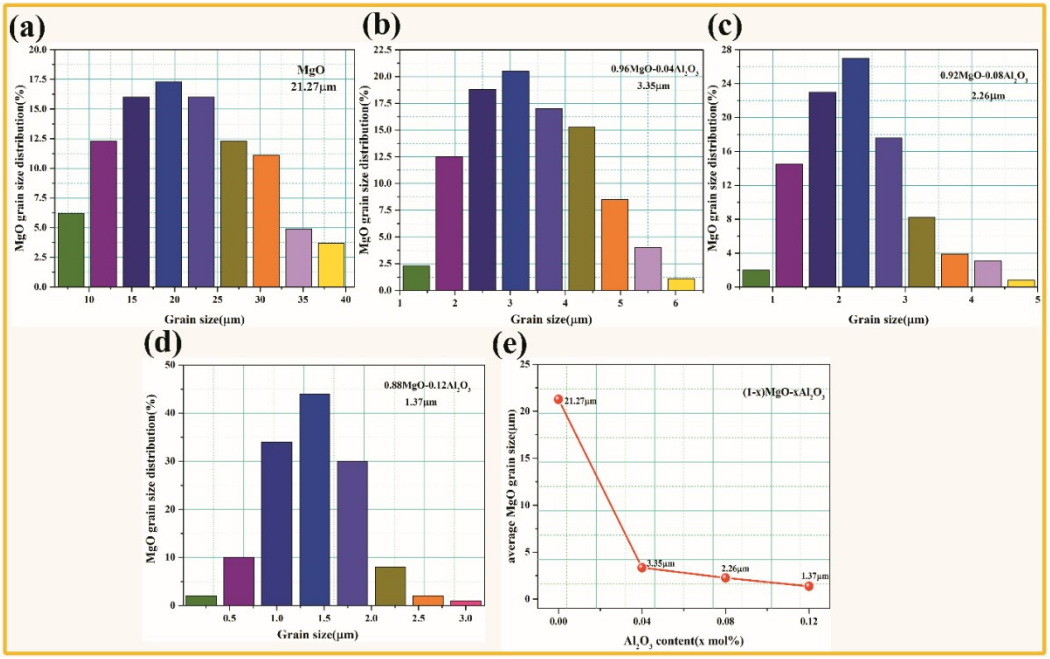


**Figure S3** Grain size distribution of (1-*x*)MgO-*x*$Al_2O_3$ ceramics: (a) MgO, (b) 0.96MgO-0.04$Al_2O_3$, (c) 0.92MgO-0.08$Al_2O_3$ and (d) 0.88MgO-0.12$Al_2O_3$. (e) Evolution of MgO average grain size in (1-*x*)MgO-*x*$Al_2O_3$ ceramics.

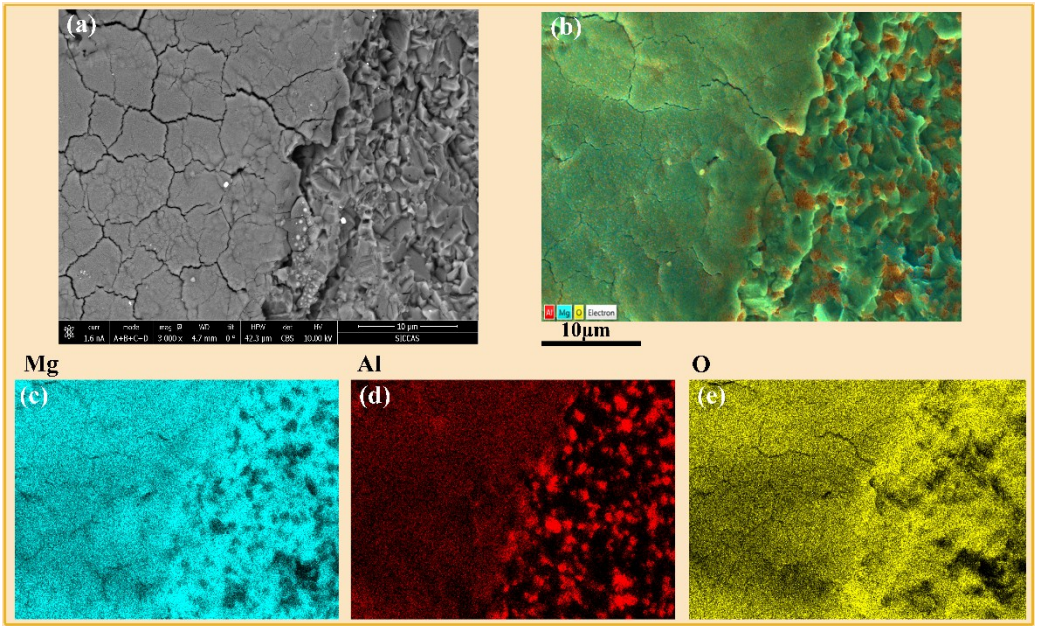


**Figure S4** SEM image (a) and EDS analysis (b)-(e) of selected area nearby dielectric breakdown channel of 0.92MgO-0.08$Al_2O_3$ ceramics.

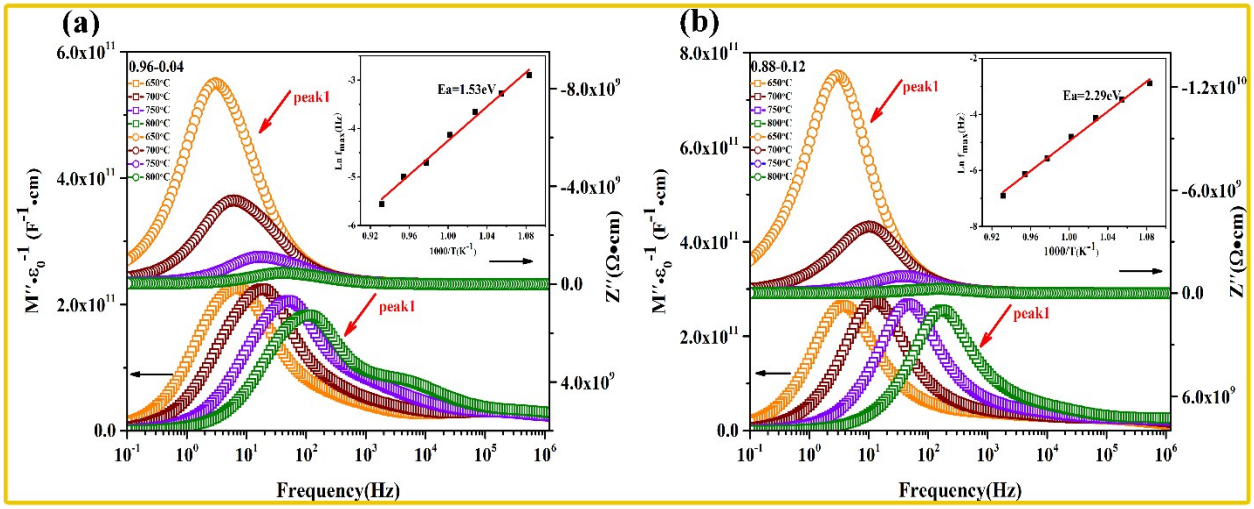


**Figure S5** Frequency dependence of Z″ and M″ tested from 650-800 °C and the inset for corresponding arrhenius plot for characteristic relaxation frequency (peak 1): (a) 0.96MgO-0.04$Al_2O_3$ and (b) 0.88MgO-0.12$Al_2O_3$.

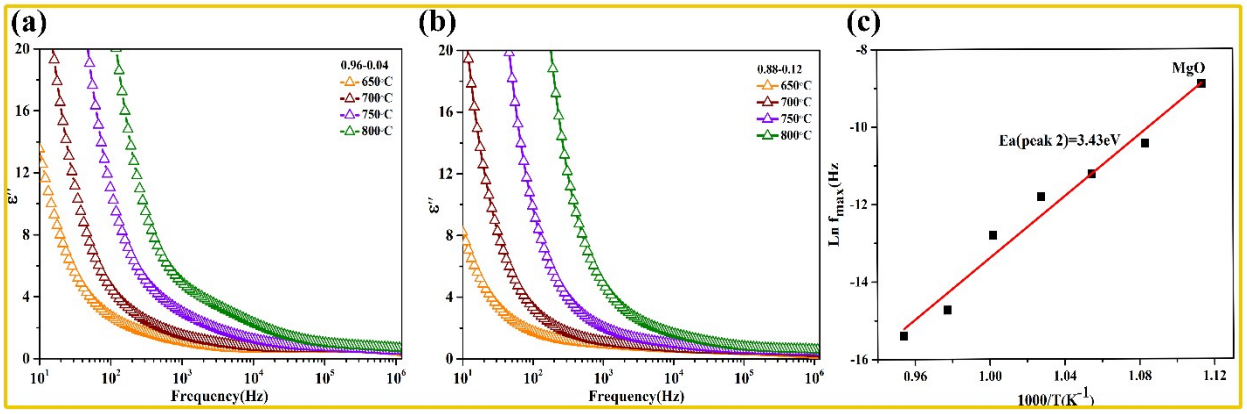


**Figure S6** Loss factor spectra measured from 650-800 °C for (a) 0.96MgO-0.04$Al_2O_3$ and (b) 0.88MgO-0.12$Al_2O_3$. (c) Arrhenius plot for characteristic relaxation frequency (peak 2) of MgO.

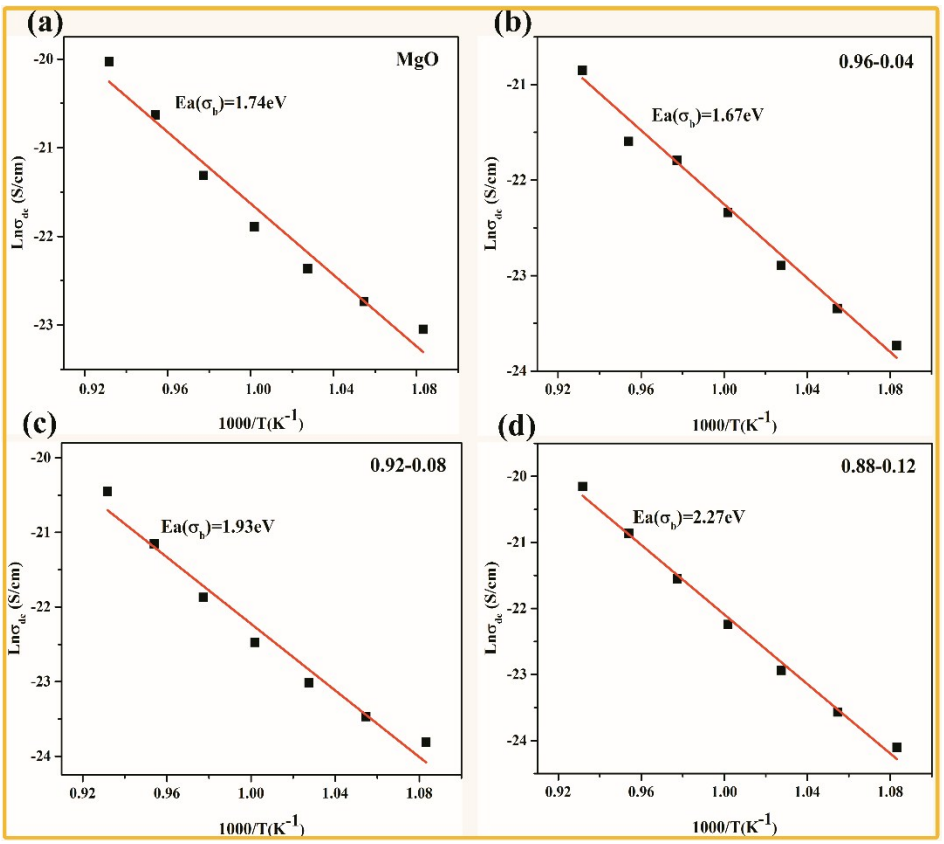


**Figure S7** Arrhenius plots for bulk conductivity (data of ac conductivity at 0.15 Hz was adopted) of (a) MgO, (b) $0.96MgO\text{-}0.04Al_2O_3$, (c) $0.92MgO\text{-}0.08Al_2O_3$ and (d) $0.88MgO\text{-}0.12Al_2O_3$

**Table S1** Chemical composition analysis of $MgCO_3 \cdot nH_2O$

| Compound | Composition (wt %) |
|---|---|
| $MgCO_3 \cdot nH_2O$ | 99.773 |
| $Al_2O_3$ | 0.125 |
| $SiO_2$ | 0.057 |
| CaO | 0.045 |

**Table S2** Comparisons of the energy storage properties of the MgO-based ceramics and other reported dielectrics.

| Materials | $E_b$ (kV cm$^{-1}$) | $W_{rec}$ (J cm$^{-3}$) | η (%) | Ref. |
|---|---|---|---|---|
| MgO | 920 | 0.45 | - | This work |
| $0.92MgO-0.08Al_2O_3$ | 1264 | 0.81 | - | This work |
| $TiO_2$-glass ceramics | 821 | 0.78 | - | [1] |
| $CaZr_{0.5}Ti_{0.5}O_3$ | 584 | 1.6 | - | [2] |
| $0.9CaTiO_3-0.1BiScO_3$ | 270 | 1.55 | 90.4 | [3] |
| $Ba_{0.4}Sr_{0.6}TiO_3$@0.08 mol$SiO_2$ | 400 | 1.6 | 90.9 | [4] |
| $0.85\ BaTiO_3-0.15Bi(Zn_{1/2}Sn_{1/2})O_3$ | 280 | 2.41 | 91.6 | [5] |
| $Na_{0.7}Bi_{0.1}NbO_3$ | 351 | 4.03 | 85.4 | [6] |
| $(Bi_{0.32}Sr_{0.42}Na_{0.2})TiO_3$/3wt%MgO | 200 | 2.09 | 84 | [7] |
| $0.58BFO-0.34BT-0.08B(Zn_{1/3}Ta_{2/3})O_3$ | 200 | 2.4 | 80 | [8] |
| $0.8K_{0.5}Na_{0.5}NbO_3-0.2Sr(Sc_{0.5}Nb_{0.5})O_3$ | 295 | 2.02 | 81.4 | [9] |
| $0.9PbHfO_3-0.1Pb(Mg_{1/2}W_{1/2})O_3$ | 151 | 3.7 | 72.5 | [10] |
| $PbHfO_3$ | 268 | 7.6 | 80.8 | [11] |
| $Ag(Nb_{0.8}Ta_{0.2})O3$ | 242 | 4.0 | 77 | [12] |
| $Ag_{0.88}Gd_{0.04}NbO_3$ | 290 | 4.5 | 64 | [13] |

Dielectrics for energy-storage usage in pulse power technology have become a research hotspot for their high energy density and fast charge-discharge performance.[14-16] For linear dielectrics, their energy storage density can be calculated by:[14]

$$J = \frac{1}{2}\varepsilon_0\varepsilon_r E^2$$

Table S2 compared the energy-storage properties of MgO-based ceramics in this work with some representative dielectrics. Compared with anti-ferroelectric and ferroelectric, the energy-storage density of linear dielectric is not high enough (only 0.81 J $cm^{-3}$ for 0.92MgO-0.08$Al_2O_3$ in this work) for their relatively low dielectric constant.[17] However, linear dielectrics usually possess high energy-storage efficiency, lower dielectric loss, outstanding dielectric stability (Fig S1b and Fig S2) and especially ultra-high dielectric breakdown strength, which enable them to have great prospect in the field of dielectric wall accelerator, microwave source generator and so on.[1, 18, 19]

**Reference**


1. Y. Huang, Y. Chen, X. Li, G. Wang, L. Xia, Y. Liu, Y. Shen, J. Shi and X. Dong, *J. Eur. Ceram. Soc.*, 2018, **38**, 3861-3866.
2. H. Y. Zhou, X. N. Zhu, G. R. Ren and X. M. Chen, *J. Alloys Compd.*, 2016, **688**, 687-691.
3. B. Luo, X. Wang, E. Tian, H. Song, H. Wang and L. Li, *ACS Appl. Mater. Interfaces*, 2017, **9**, 19963-19972.
4. Y. H. Huang, Y. J. Wu, B. Liu, T. N. Yang, J. J. Wang, J. Li, L.-Q. Chen and X. M. Chen, *J. Mater. Chem. A*, 2018, **6**, 4477-4484.
5. M. Zhou, R. Liang, Z. Zhou and X. Dong, *J. Mater. Chem. C*, 2018, **6**, 8528-8537.
6. M. Zhou, R. Liang, Z. Zhou and X. Dong, *J. Mater. Chem. A*, 2018, **6**, 17896-17904.
7. F. Li, X. Hou, J. Wang, H. Zeng, B. Shen and J. Zhai, *J. Eur. Ceram. Soc.*, 2019, **39**, 2889-2898.
8. N. Liu, R. Liang, Z. Zhou and X. Dong, *J. Mater. Chem. C*, 2018, **6**, 10211-10217.
9. B. Qu, H. Du and Z. Yang, *J. Mater. Chem. C*, 2016, **4**, 1795-1803.
10. P. Gao, Z. Liu, N. Zhang, H. Wu, A. A. Bokov, W. Ren and Z.-G. Ye, *Chem. Mater.*, 2019, **31**, 979-990.
11. J. Wei, T. Yang and H. Wang, *J. Eur. Ceram. Soc.*, 2019, **39**, 624-630.
12. L. Zhao, Q. Liu, J. Gao, S. Zhang and J. F. Li, *Adv Mater*, 2017, **29**.
13. S. Li, H. Nie, G. Wang, C. Xu, N. Liu, M. Zhou, F. Cao and X. Dong, *J. Mater. Chem. C*,

2019, **7**, 1551-1560.

14. Z. Yao, Z. Song, H. Hao, Z. Yu, M. Cao, S. Zhang, M. T. Lanagan and H. Liu, *Adv Mater*, 2017, **29**.
15. J. Li, F. Li, Z. Xu and S. Zhang, *Adv Mater*, 2018, **30**, e1802155.
16. C. Xu, Z. Fu, Z. Liu, L. Wang, S. Yan, X. Chen, F. Cao, X. Dong and G. Wang, *ACS Sustainable Chem. Eng.*, 2018, **6**, 16151-16159.
17. X. Hao, *J. Adv. Dielectr.*, 2013, **03**.
18. S. Sampayan, G. Caporaso, Y. Chen, S. Hawkins, C. Holmes, M. Krogh, J. McCarrick, S. Nelson, W. Nunnally, B. Poole, M. Rhodes, D. Sanders, K. Selenes, J. Sullivan, L. Wang and J. Watson, presented in part at the 2005 IEEE Pulsed Power Conference, CA,USA, June 2005.
19. Y. Shen, W. Wang, Y. Liu, L. Xia, H. Zhang, H. Pan, J. Zhu, J. Shi, L. Zhang and J. Deng, *Rev. Sci. Instrum.*, 2015, **86**.